Flexible GelSight Sensor Design for shape classification and force estimation

Vinod Ram Keertana[1], Kai Long[1], Pohekar Aditi[1], Senthil Kumar Kirthika[1], Lalithkumar Seenivasan[1] and Hongliang Ren[1]*

[1]*Department of Biomedical Engineering, National University of Singapore, Singapore 117583, Singapore*

***Abstract*— The tactile properties of a tissue such as hardness, texture, shape, are important for surgical procedures. While this information is obtained effortlessly during an open surgery, in a minimally invasive endoscopic surgery this is compromised. There are several developments in the tactile sensing field but lack the flexibility required for use in endoscopy. This paper discusses the implementation of pliability using two different origami structures with tactile sensing ability of a traditional GelSight sensor. Additionally, markers are added on the surface of the sensor for contact force estimation. The two origami structures square origami bellow and twisted paper column are compared for their stability and compliance to the application. The twisted paper column is concluded to have higher stability and greater application. The data collected from these prototypes are processed and classification of 4 different shapes and force estimation for 5 different classes are obtained.**

***Index Terms*—Actuator, Artificial intelligence, Awareness, Endoscopy, Soft robotics, Tactile sensor**

I. INTRODUCTION

ENDOSCOPY refers to a minimally invasive procedure in which a slender tubular optical instrument is inserted inside the body to examine internal organs. Endoscopic procedures can be performed by inserting the endoscopic tubes into the body either through natural orifices like nostril, mouth, anus etc. or through small incisions [1], [2]. This procedure caters to various needs such as diagnosis, tumor removal, tissue biopsy, stent placements etc. with surgery being a major application. Due to its minimally invasive nature, use of this technology in surgery offers a lot of advantages, like relatively low risk of infection, faster recovery of the patients and less scarring. However, endoscopic minimally invasive surgery (MIS) is challenging as compared to the traditional methods. First, the tactile sensibility of the operating environment is compromised [3], [4]. Tactile feedback is very important during tool-tissue interaction as it enables the surgeon to apply force in an appropriate manner, so as to prevent any damage to the healthy tissues and helps in the characterization of the contacted tissues[5], [6], [7]. Thus, there is a need for tactile feedback. Second, the space constraint of the operating environment during the endoscopic procedure. The entry point is usually small in the form of a natural orifice or a key-hole incision and the track followed by the endoscope is narrow and tortuous. Therefore, the shaft design is expected to be slender and flexible. The aim of this paper is to present a proof of concept for a flexible setup with tactile capabilities.

II. RELATED WORKS

A. Tactile sensors

The hardness of objects without restrictions in force applied and surface geometry was measured [8]. It worked on the principle of image processing of image captured from the elastomeric material to obtain brightness and radius values to determine hardness. The estimation was done only on silicone spherical shapes which indicated limitation in shape of sample. A methodology was proposed to determine the topography of tissues and different properties of tissues such as tumors[9]. This work mainly involve the usage of deep learning and machine learning models like General Adversarial Network (GAN) and Convolutional Neural Network (CNN). The distance between the camera and sensing material was comparatively big and cumbersome in its architecture. Another model was proposed for estimation of hardness using a tactile sensor based on frequency shift during the vibration of piezoelectric element [10]. The methodology uses a mathematical model to determine the frequency shift and uses a one-way ANOVA model and multiple regression model for statistical data analysis. This paper indicates how different tissue compositions could indicate a disease possibility. The only disadvantage being the invasiveness and the paper indicates further miniaturization of size. Shogo Okamoto et al. came up with a soft tactile sensor that gives the estimate of characteristics like roughness, friction, and hardness of samples [5]. The experiment also involves calculation of young's moduli of 3 samples using a strain gauge. This method was successful in obtaining sample's spatial wavelength and was also the first tactile sensing unit to give real time quick sensing information. In this proposal however, the load or force applied is limited and the sample shapes used are limited. The model by Mike Lambeta et al. is the most recent development in the tactile sensing devices [11]. It uses machine learning models for training. Feature maps are obtained from the images captured in the camera which are then encoded to obtain positions and intensity details. With these developments in the field of tactile sensing, our proposal aims at increasing the flexibility of a tactile sensor along with usage of an endoscope camera set-up with appropriate illumination to obtain image with sufficient resolution and clarity.

B. Origami inspired patterns

Origami offers properties like scale-independence and flexibility which come across as very helpful in this context. Origami-inspired robotics is being used for various applications like manipulation, locomotion, gripping etc. The structures can be broadly divided into two types, i)

Tessellation, i.e. single sheet structure, ii) Modular. The twisted tower structure, is highly flexible and also can be analyzed by using rigid body dynamics [12]. Origami magic ball based cylinder proposed in [13] is a modular structure with magic ball/ water bomb as a single unit, is again highly flexible. However, cumbersomeness of the two structures due to the multiple folding creases, is a major drawback. Chen et al. discussed diagonal pattern based twisted paper column, which is a single sheet structure which offers linear displacement in the vertical direction with a twisted opening and closing action [14]. Butler et al. proposed accordion pattern based origami bellows structure, which is again a single sheet structure, but assembled in a way to offer three DOFs [15]. Thus, it's simple and highly flexible at the same time.

Hence, several origami-inspired structures are evaluated on the basis of simplicity and flexibility, in order to design a suitable structure for the shaft of the proposed tactile sensor.

III. TACTILE SENSOR ARCHITECTURE

A. *System Overview*

Figure 1 represents the various components of the telescopic harness sensor. The top layer possesses the incision for endoscopic camera. The intermediate shaft is composed of adjustable flexible origami sleeve with additional illumination set-up with Light-emitting diodes (LED). The bottom layer consists of stretchable elastomeric membrane with optical markers.

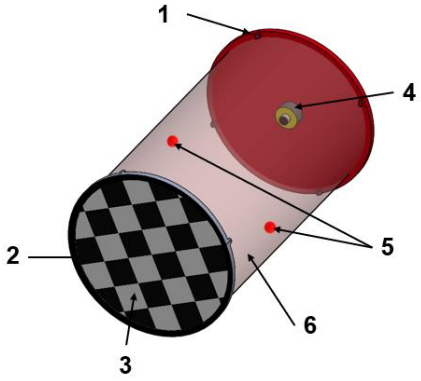

Figure 1 Structure of the telescopic harness sensor

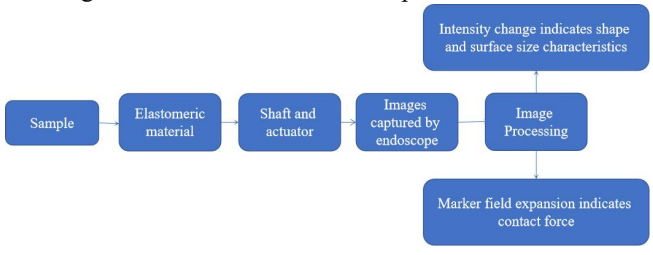

Figure 2 Information flow of the hardness sensor

B. *Optical perception*

The optical perception (awareness) deals with capturing images of the elastomeric material. The most important aspect for perception of good quality images is illumination. In order to obtain the ideal illumination, the light source should meet the requirements of sufficient and adjustable brightness and stay inert to the surrounding light. To satisfy this criteria, we used two illumination methods, one is the adjustable light source that comes with the endoscope placed opposite to the elastomer (Figure 3), the other is LEDs of two different wavelengths placed at the lateral edges of the sensor (Figure 4). These LEDs are used to avoid overexposure of vertical light from the endoscope. The dataset was collected with minimum illumination from endoscope and maximum illumination from the LEDs power by a 2V DC power supply. The elastomeric material used is the second important aspect of awareness. The material used is ecoflex which is extensively used in tactile applications because of its low viscosity and high stretchability. The elastomeric material covers up to an area of 7 cm^2. The material is then marked with black industrial paint markers.

Figure 3 Endoscope camera with adjustable brightness

Figure 4 LEDs in the middle of the origami sleeve

C. Telescopic shaft

For the current application, the origami structures used are single sheet structures, i) accordion pattern based square bellows and ii) diagonal pattern based collapsible paper column, due to the simplicity and slickness these structures offer. The two structures are compared on two aspects, strain visualization and degrees of freedom.

Strain Visualization

Strain visualization for the two structures is done using origamisimulator.org [16], as shown in Figure 5. The simulator approximates the engineering/Cauchy strain across the origami sheet and maps it to a color. From the strain visualization simulation, it can be said that for the same percentage of folding, collapsible paper column displays more strain values, and hence provides more displacement as compared to the bellow structure.

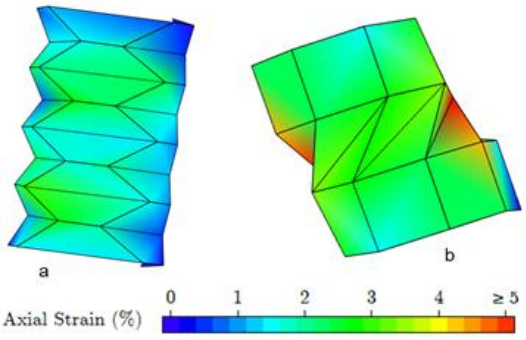

Figure 5 Strain visualization for the two structures

Degrees of freedom

In an ideal case scenario, we may assume that each crease will have uniform folding. However, the creases and folds are prone to human error, which makes the motion uncertain and difficult to control. It is intuitive that more creases could add more uncertainty. Thus, this section aims at evaluating the number of DOFs of both the origami structures. The degrees of freedom of a 3-D origami can be defined as represented in Eqn1 [17]:

$$DOF = NE0 - 3NL - 3 \text{ ----------1}$$

where, NE0 is the number of edges on the boundary and NL number of holes [18]. Using this formula, the paper column structure has 14 DOFs while the bellow structure has 5. This theoretically validates that the paper column structure is more stable and easier to control.

D. Image processing algorithm

The image once captured by the camera, is processed to obtain the details regarding tissue hardness. Image processing enables us to obtain properties of the tissue from preliminary values of intensity and marker area expansion in the image captured. Here, the technique of obtaining the surface normal characteristics and shape characteristics of the sample by observing the brightness/intensity change in the image is used [4]. The brightness change is directly proportional to the hardness of the surface, the brightness in the image increases for harder objects when force is applied [4]. Thus, the intensity value is an important parameter obtained from the image captured. A marker field is added on the surface of the elastomeric material to observe the surface indentation of the elastomer when force is applied on the sample. The expansion in the marker field is directly proportional to the contact force between the elastomeric material and the sample. It is learned that harder objects increase the indentation, further concluding that the distance between the markers increases with increase in force applied [4].

IV. Data Collection and Processing

A. Data Collection

Shape classification

Figure 6 represents the two prototypes (a) square bellow and (b) collapsible paper column prototype which are used for the data collection for shape classification. 3 different 3D printed structures of the material PLA (Polylactic acid) represented in Figure 7 are used to obtain images of 4 different shapes namely square, rectangle, circle, triangle. The images obtained with an endoscope from these incident shapes are shown in Figure 8. The camera captures images with a resolution of 640x480 pixels.

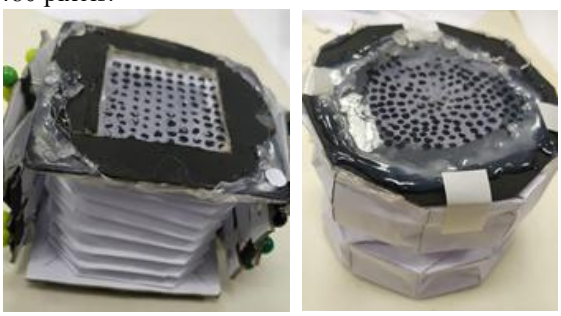

Bellow prototype Paper column prototype

Figure 6 Structure of two prototypes

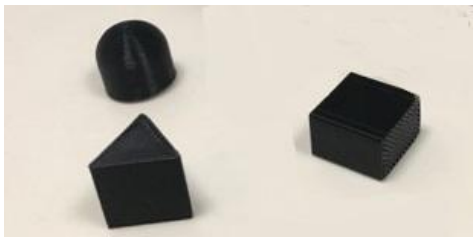

Figure 7 3D printed different shapes

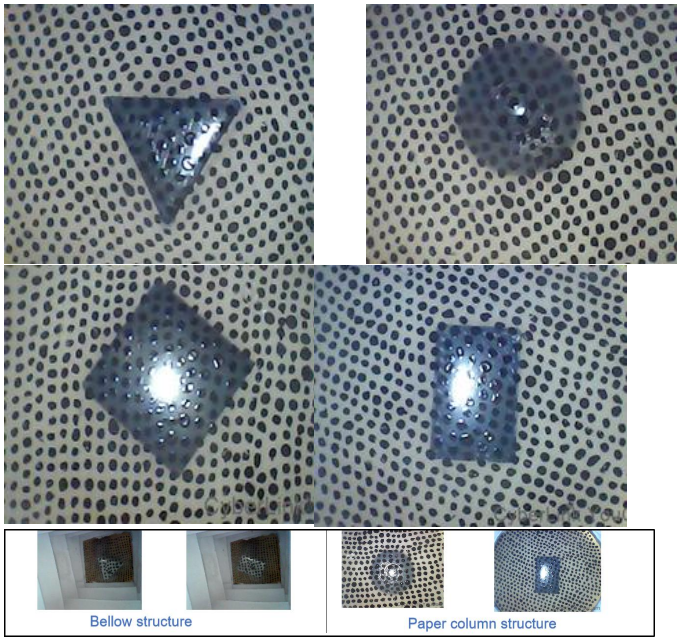

Figure 8 Shape classification images

Force estimation

The data collection for force estimation is done with the Instron universal testing machine (UTM) which has a force testing capacity range from as low as 0.02N to as high as 50kN. The data was captured using a loadcell with a capacity of 100N. The setup for this data collection is as represented in the Figure 9 with the force applied vertically on the object which is placed on top of the elastomeric material. The data is collected from the collapsible paper column prototype. The experiment was done such that different images were captured, at the same time taking down the absolute force values shown on the software. The data is collected from 13 different locations capturing images for 5 different values of force (0N, 0.1N, 0.2N, 0.3N, 0.5N) at each location. Figure 10 shows only one group.

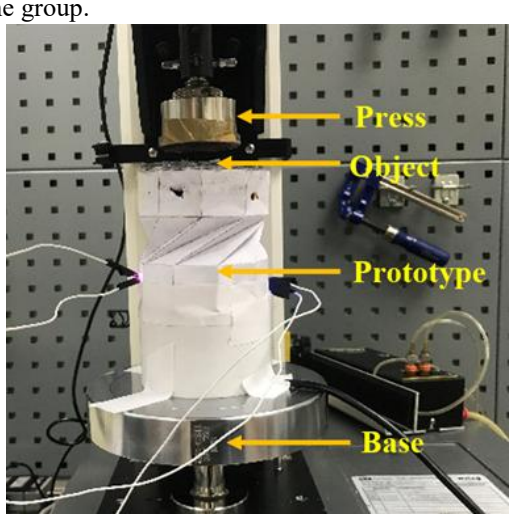

Figure 9 Setup of force estimation

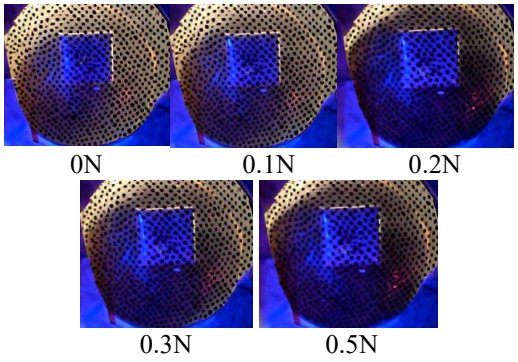

Figure 10 Force estimation images

B. Shape Classification

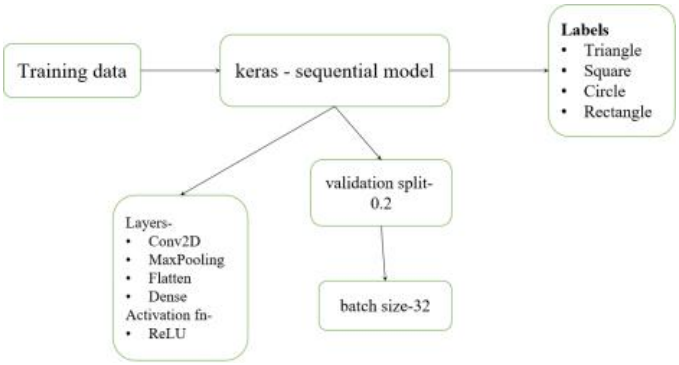

Figure 11 Algorithm for shape classification

A keras sequential model for shape classification is used in the google Colab notebook, as shown in Figure 11. Different training and validation data are used for the two different prototypes. The images used for the training of the modules are a set of six images captured at different depths from both the paper column prototype and the bellow prototype for four different labels namely- square, circle, rectangle and triangle. A standard data set of shapes is also used from the Kaggle dataset for the square, circle, and triangle shapes. For the previously unavailable dataset of a rectangle, binary images of rectangles are created with OpenCV and used for training. Hence 100 standard images and 6 collected images are used for the training of the model making it 106 images per class. A 2D CNN sequential model is used which is generally used for classification of images [19]. The different layers of the model used are Convolution 2D, MaxPooling 2D, Flatten, Dense and Dropout. The kernel size used for the convolution layers is 3x3 and the input shape is also defined. Finally, the model is compiled and trained to obtain a training and validation accuracy graph as represented in Figure 12 where the accuracy increases with the number of epochs and the loss decreases. Here, the shape of the sample is classified into square, rectangle, triangle, and Circle.

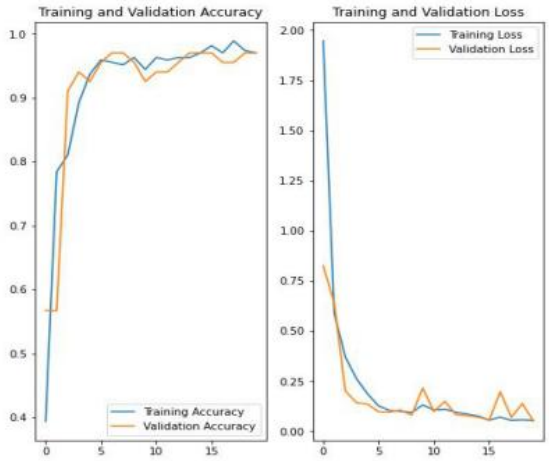

Figure 12 Graph of training and validation accuracy of Shape classification CNN model.

C. *Force Estimation*

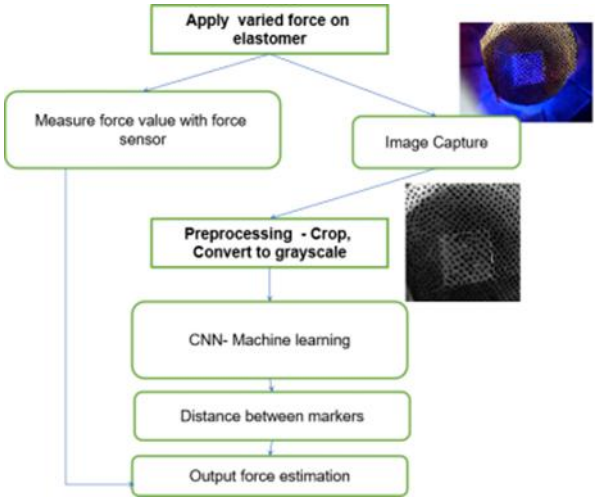

Figure 13 Algorithm for force estimation

The images are captured for 5 different classes of data with forces of 0N, 0.1N, 0.2N, 0.3N, 0.5N. These values of force are applied at 13 different locations capturing a total of 65 images. These images are used for training of the CNN keras sequential model. The data in this case are not augmented because the orientation of the markers changes, which leads to inaccurate training of the model. The markers if drawn mechanically maintaining equidistance will be constant throughout the surface and the data can be augmented for better training and efficiency. The images are captured with illumination from 2 LED's on lateral edges, which can also lead to minute variation in the intensity of the images during the data collection. To eradicate this error the images are preprocessed before training. The preprocessing involves cropping of the image to remove the area other than the sensor area and conversion to grayscale as indicated in Figure 13. After sufficient preprocessing, the model is assumed to be trained by the distance between the markers. The property of expansion in the marker field indicating the contact force applied serves as the main principle of force estimation [20]. After training the model, it is then validated with a 0.2 split in the data and the accuracy of training and validation is as shown in Figure 14. The figure shows fluctuations in the accuracy due to human error in marking of the elastomeric field and slight intensity variations which can be eradicated with further work.

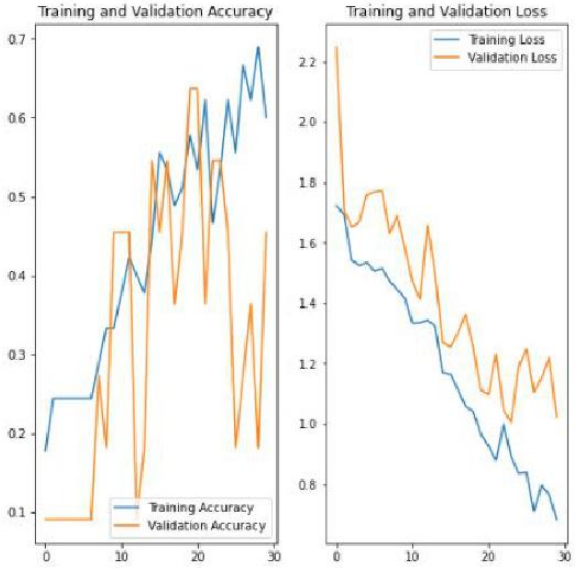

Figure 14 Graph of training and validation accuracy of Force classification CNN model.

V. RESULTS AND DISCUSSION

In this article, we compared two different origami structures square bellow and collapsible paper column. The theoretical calculation of degrees of freedom and preliminary shape data collected show that the collapsible paper column is comparatively more stable and can be used in the applications with endoscopy. The experimentation shows that the elastomeric membrane in both the structures deform when a force is applied to it, and marker field displacement is observed. From the output of the machine learning algorithm, we conclude that the model is able to obtain shape classification of 4 different structures and classify the force into 5 different classes. The paper column structure shows bistability having two stable states, the fully stable closed (collapsed) state and the partially stable open state which is stable till a force of 1N is applied following which the structure collapses. In real time applications the force applied can be increased with a studier prototype and hence can be used on tissues.

VI. CONCLUSION

The proposal therefore concludes that in terms of accuracy and stability, the collapsible paper column is fundamentally better. The comparison between two types of illumination indicated better image capture with lateral illumination from LEDs of two different wavelengths to avoid the loss of marker patterns. The paper hence shows the use of flexible origami soft robotics in applications involving the tactile sensing which can be used in biomedical industries and also in other

manufacturing industries by making a couple of changes to the Neural network models. The methodology currently used for shape classification and force estimation can also be further extended for obtaining other tactile properties.

VII. Future Work

The proposed design can have a major impact on improving the safety and effectiveness of the endoscopic surgical procedure. Currently, we have demonstrated the proof of concept using a paper model of dimensions in the cm scale. However, in the future, the structure can be miniaturized, as origami structure is size-invariant. Further, the material can be changed to a biocompatible and sturdier counterpart. Another aspect which can be added is automated actuation to facilitate the navigation inside the body. On the AI front, a larger dataset can be used to achieve better machine learning accuracy. In this paper we have demonstrated shape classification and force estimation. These two parameters can be implemented with an appropriate mathematical model to obtain hardness of the structure. Yi et al. has achieved this for spherical objects [9]. As discussed in [21], [22], [23] origami structures are used in a lot of navigational robotics applications. The concept proposed in this paper can be used to add tactile sensing capabilities to these robots.

Acknowledgment

Sponsor and financial support acknowledgments are placed in the unnumbered footnote on the first page, not here.

References

[1] A. Hamed *et al.*, "Advances in Haptics, Tactile Sensing, and Manipulation for Robot-Assisted Minimally Invasive Surgery, Noninvasive Surgery, and Diagnosis," *Journal of Robotics*, Dec. 31, 2012. https://www.hindawi.com/journals/jr/2012/412816/ (accessed Sep. 22, 2020).

[2] O. A. J. van der Meijden and M. P. Schijven, "The value of haptic feedback in conventional and robot-assisted minimal invasive surgery and virtual reality training: a current review," *Surg. Endosc.*, vol. 23, no. 6, pp. 1180–1190, Jun. 2009, doi: 10.1007/s00464-008-0298-x.

[3] Jun Ueda, Y. Ishida, M. Kondo, and T. Ogasawara, "Development of the NAIST-Hand with Vision-based Tactile Fingertip Sensor," in *Proceedings of the 2005 IEEE International Conference on Robotics and Automation*, Apr. 2005, pp. 2332–2337, doi: 10.1109/ROBOT.2005.1570461.

[4] A. Yamamoto, S. Nagasawa, H. Yamamoto, and T. Higuchi, "Electrostatic tactile display with thin film slider and its application to tactile telepresentation systems," *IEEE Trans. Vis. Comput. Graph.*, vol. 12, no. 2, pp. 168–177, Mar. 2006, doi: 10.1109/TVCG.2006.28.

[5] S. Okamoto, M. Konyo, Y. Mukaibo, T. Maeno, and S. Tadokoro, "Real-time Estimation of Touch Feeling Factors Using Human Finger Mimetic Tactile Sensors," in *2006 IEEE/RSJ International Conference on Intelligent Robots and Systems*, Oct. 2006, pp. 3581–3586, doi: 10.1109/IROS.2006.281648.

[6] S. Zhao, D. Parks, and C. Liu, "Design and Modeling of a Wide Dynamic-Range Hardness Sensor for Biological Tissue Assessment," *IEEE Sens. J.*, vol. 13, no. 12, pp. 4613–4620, Dec. 2013, doi: 10.1109/JSEN.2013.2271736.

[7] L. Zhang, F. Ju, Y. Cao, Y. Wang, and B. Chen, "A tactile sensor for measuring hardness of soft tissue with applications to minimally invasive surgery," *Sens. Actuators Phys.*, vol. 266, pp. 197–204, Oct. 2017, doi: 10.1016/j.sna.2017.09.012.

[8] W. Yuan, S. Dong, and E. H. Adelson, "GelSight: High-Resolution Robot Tactile Sensors for Estimating Geometry and Force," *Sensors*, vol. 17, no. 12, Art. no. 12, Dec. 2017, doi: 10.3390/s17122762.

[9] L. J. Yi, L. Seenivasan, and K. Kumar, "Deep Learning Based Depth Mapping, Classification And Force Estimation For Haptic Vision," p. 15.

[10] A. Eklund, A. Bergh, and O. A. Lindahl, "A catheter tactile sensor for measuring hardness of soft tissue: measurement in a silicone model and in anin vitro human prostate model," *Med. Biol. Eng. Comput.*, vol. 37, no. 5, pp. 618–624, Sep. 1999, doi: 10.1007/BF02513357.

[11] M. Lambeta *et al.*, "DIGIT: A Novel Design for a Low-Cost Compact High-Resolution Tactile Sensor With Application to In-Hand Manipulation," *IEEE Robot. Autom. Lett.*, vol. 5, no. 3, pp. 3838–3845, Jul. 2020, doi: 10.1109/LRA.2020.2977257.

[12] K. Lee, Y. Wang, and C. Zheng, "TWISTER Hand: Underactuated Robotic Gripper Inspired by Origami Twisted Tower," *IEEE Trans. Robot.*, vol. 36, no. 2, pp. 488–500, Apr. 2020, doi: 10.1109/TRO.2019.2956870.

[13] A. A. Abtan, "Design and Fabrication of Origami Elements for use in a Folding Robot Structure," p. 160.

[14] Y. Chen, J. Yan, and J. Feng, "Geometric and Kinematic Analyses and Novel Characteristics of Origami-Inspired Structures," *Symmetry*, vol. 11, no. 9, Art. no. 9, Sep. 2019, doi: 10.3390/sym11091101.

[15] J. Butler *et al.*, "Highly Compressible Origami Bellows for Harsh Environments," in *Volume 5B: 40th Mechanisms and Robotics Conference*, Charlotte, North Carolina, USA, Aug. 2016, p. V05BT07A001, doi: 10.1115/DETC2016-59060.

[16] "Origami Simulator." https://origamisimulator.org/ (accessed Nov. 06, 2020).

[17] Y. Zhao, Y. Kanamori, and J. Mitani, "Design and motion analysis of axisymmetric 3D origami with generic six-crease bases," *Comput. Aided Geom. Des.*, vol. 59, pp. 86–97, Jan. 2018, doi: 10.1016/j.cagd.2017.10.002.

[18] T. Tachi, "Geometric Considerations for the Design of Rigid Origami Structures," p. 12, 2010.

[19] H. A. Atabay, "BINARY SHAPE CLASSIFICATION USING CONVOLUTIONAL NEURAL NETWORKS," vol. 7, p. 5, 2016.

[20] T. Assaf, C. Roke, J. Rossiter, T. Pipe, and C. Melhuish, "Seeing by Touch: Evaluation of a Soft Biologically-Inspired Artificial Fingertip in Real-Time Active Touch," *Sensors*, vol. 14, no. 2, Art. no. 2, Feb. 2014, doi: 10.3390/s140202561.

[21] T. Manwell, B. Guo, J. Back, and H. Liu, "Bioinspired setae for soft worm robot locomotion," *2018 IEEE Int. Conf. Soft Robot. RoboSoft*, 2018, doi: 10.1109/ROBOSOFT.2018.8404896.

[22] L. Paez, G. Agarwal, and J. Paik, "Design and Analysis of a Soft Pneumatic Actuator with Origami Shell Reinforcement," 2016. /paper/Design-and-Analysis-of-a-Soft-Pneumatic-Actuator-Paez-Agarwal/26832dc37dab021a4c61c90e2496d6c7c65bfca8 (accessed Nov. 08, 2020).

[23] A. Pagano, T. Yan, B. Chien, A. Wissa, and S. Tawfick, "A crawling robot driven by multi-stable origami," *Smart Mater. Struct.*, vol. 26, no. 9, p. 094007, Sep. 2017, doi: 10.1088/1361-665X/aa721e.